

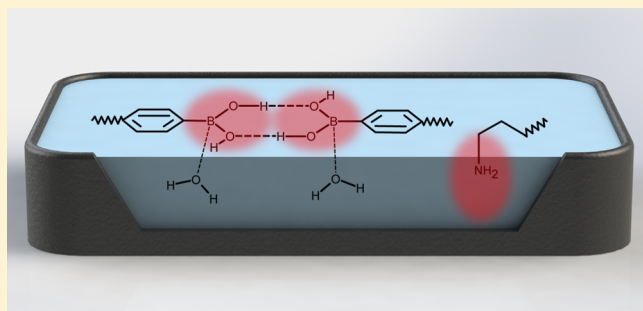
Surface Behavior of Boronic Acid-Terminated Silicones

Erum Mansuri,[†] Laura Zepeda-Velazquez,[‡] Rolf Schmidt,[†] Michael A. Brook,^{*,‡} and Christine E. DeWolf^{*,†}[†]Department of Chemistry and Biochemistry and Concordia Centre for NanoScience Research, Concordia University, 7141 Sherbrooke Street West, Montréal, Québec H4B 1R6, Canada[‡]Department of Chemistry and Chemical Biology, McMaster University, 1280 Main Street West, Hamilton, Ontario L8S 4M1, Canada

Supporting Information

ABSTRACT: Silicone polymers, with their high flexibility, lie in a monolayer at the air–water interface as they are compressed until a critical pressure is reached, at which point multilayers are formed. Surface pressure measurements demonstrate that, in contrast, silicones that are end-modified with polar groups take up lower surface areas under compression because the polar groups submerge into the water phase. Boronic acids have the ability to undergo coordination with Lewis bases. As part of a program to examine the surface properties of boronic acids, we have prepared boronic acid-modified silicones (SiBAs) and examined them at the air–water interface to better understand

if they behave like other end-functional silicones. Monolayers of silicones, aminopropylsilicones, and SiBAs were characterized at the air–water interface as a function of end functionalization and silicone chain length. Brewster angle and atomic force microscopies confirm domain formation and similar film morphologies for both functionalized and non-functionalized silicone chains. There is a critical surface pressure (10 mN m^{-1}) independent of chain length that corresponds to a first-order phase transition. Below this transition, the film appears to be a homogeneous monolayer, whose thickness is independent of the chain length. Ellipsometry at the air–water interface indicates that the boronic acid functionality leads to a significant increase of film thickness at low molecular areas that is not seen for non-functionalized silicone chains. What differentiates the boronic acids from simple silicones or other end-functionalized silicones, in particular, is the larger area occupied by the headgroup when under compression compared to other or non-end-functionalized silicones, which suggests an in-plane rather than submerged orientation that may be driven by boronic acid self-complexation.



INTRODUCTION

An important consequence of the highly flexible Si–O backbone of silicone polymers is an intrinsically low surface energy and high surface activity. When further modified with hydrophilic groups, silicone surfactants have applications ranging from agricultural adjuvants¹ to foam stabilizers in polyurethane.² While polyethers are frequently the hydrophiles of choice, silicones bearing other surface-active groups, including phosphates, sulfates,³ amines, carboxylic acids, and amino acids,^{4,5} have been developed for specific applications, particularly in personal care applications. The surface activities of some of these materials can be modified at pH values away from neutrality, however, usually at conditions under which the silicones are known to undergo depolymerization.

The interfacial behavior of silicone polymers [typically poly(dimethylsiloxane) (PDMS)], including a range of end-functionalized PDMS, has been widely studied.^{2,6–10} At high molecular areas, PDMS chains are generally assumed to adopt a caterpillar conformation, where molecules are stretched and lying at the water surface with the siloxane backbone immersed

in the aqueous subphase and the methyl groups extending into the air. As the molecular area is reduced, molecules are forced to come into contact with one another and adopt a zigzag conformation, where the backbone becomes less-solvated as some oxygen and silicon atoms are no longer in contact with water.⁷ Further compression leads to a phase transition. In early work, Lenk et al.⁹ proposed the formation of helices during this phase transition for both functionalized and non-functionalized PDMS. Later work on PDMS by Kim et al.⁷ suggested a multilayering rather than helix formation on the basis of vibrational sum frequency spectroscopy measurements. It is now generally accepted that the chains slide above one another and form odd numbered multilayers. If they do form helices, it is most likely that the helices form on top of a monolayer and not just directly at the air–water interface.^{7,11}

Received: June 11, 2015

Revised: July 21, 2015



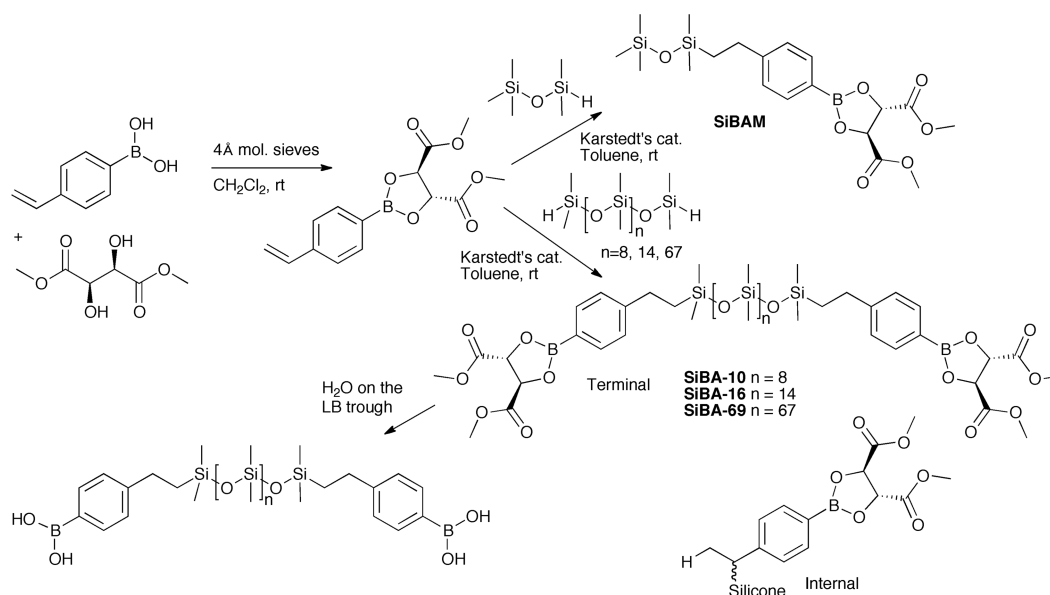


Figure 1. Chemical synthesis and structure of boronic acid-functionalized silicones. The ratio of terminal/internal isomers in the SiBAs is $\sim 70:30$. The abbreviated name indicates the total number of silicon atoms in the central silicone block (i.e., SiBA-10; $n = 8$).

Table 1. Details of the Functionalized Silicones Used in These Studies

	End Group*	m	n	M_n (g mol ⁻¹)	Trade Name
SiBA-10		10	8	~ 1310	-
SiBA-16		16	14	~ 1750	-
SiBA-69		69	67	~ 5680	-
H-PDMS-10	H	10	8	~ 650	DMS-H03
H-PDMS-16		16	14	~ 1100	DMS-H11
H-PDMS-69		69	67	~ 5030	DMS-H21
H₂N-PDMS-10		10	8	~ 840	DMS-A11
SiBAM		2	-	~ 296	-

*Note that the terminal and internal isomers are formed in a $\sim 70:30$ ratio.²

The impact of end functionalization of both PDMS and carbon-based backbone polymers has also been studied at the air–water interface.^{9,12} Functional groups typically serve to anchor the chain to the subphase, forcing a more horseshoe-type conformation, as also reported for long-chain bolaform amphiphiles.¹³ The strength of this type of anchoring has been shown to impact the surface pressure at small molecular areas and the surface pressure at film collapse.^{9,12}

Boronic acids are known to provide a pH-sensitive binding site for diols, specifically the 1,2- and 1,3-diols that are common in saccharides. The binding affinity for different diol-containing compounds varies significantly (over orders of magnitude), which enables differentiation of sugars.¹ On the basis of this selective binding, boronic acids have been proposed as drug delivery agents,¹⁴ artificial lectins,¹⁵ and tunable saccharide sensors.^{16,17} Any changes to the local environment at boron can

be “locked in” by forcing the boron center to tetracoordination, for example, at higher pH.

Recently, we reported the preparation of boronic acid-modified silicone polymers.^{18,19} The surface activity of boronic acids at the air–water interface has been reported to be affected by the size and structure of boronate.^{20–22} Silicone boronic acid polymer behavior should be tunable by modification of the subphase constituents, including pH, presence of sugars, etc., under conditions that do not affect the silicone backbone. That is, unlike other silicone-based surfactants, it should be possible to dynamically modify the interfacial behavior of silicone boronic acids under mild conditions. This paper describes an initial study on the behavior of silicone boronates at the air–water interface compared to related surface-active silicone polymers, which will allow for specific applications to be identified. The silicone boronates under consideration are α,ω -boronic acid-functionalized silicones (Figure 1) of various

molecular weights that were examined as a function of chain length, pH, and temperature.

EXPERIMENTAL SECTION

Materials. Boronic acid-terminated PDMS (difunctional SiBAs and monofunctional SiBAM; Figure 1) were synthesized as previously described.¹⁹ The hydride-terminated silicone precursors, (H-PDMS-*m*, where *m* = number of silicon atoms in the chain, 10, 16, or 69) and aminopropyl-terminated polydimethylsiloxane (H₂N-PDMS-10; *m* = 10) were obtained from Gelest, Inc. (Morrisville, PA). Details of the functionalized silicones are provided in Table 1. The average number of repeat units and corresponding molecular weights were determined by ¹H nuclear magnetic resonance (NMR).

Spreading solutions were prepared in chloroform [high-performance liquid chromatography (HPLC) grade, Fisher Scientific], with concentrations ranging from 0.5 to 1 mM. All solutions were stored at −4 °C and brought to room temperature before use. Ultrapure water with a resistivity of 18.2 MΩ cm was obtained from an EasyPure II LF system (Barnstead, Dubuque, IA). Silicon wafers were purchased from Wafer World, Inc. (West Palm Beach, FL) and cleaned using the following procedure: substrates were immersed in a 1:1 mixture of concentrated hydrochloric acid [American Chemical Society (ACS) grade, EM Science] and methanol (HPLC grade, Fisher Scientific) for 30 min, rinsed abundantly with ultrapure water, immersed in concentrated sulfuric acid (reagent grade, J.T. Baker) for 30 min, rinsed abundantly with ultrapure water, and stored in ultrapure water. Storage times never exceeded 7 days. Prior to use, silicon substrates were blown dry with nitrogen. Mica sheets were purchased from Ted Pella, Inc. (Redding, CA) and were cleaved by separating thin layers from either side of the sheet to expose a clean surface for deposition.

Methods. Surface pressure–area isotherms were obtained on thermostated Langmuir film balances (140 cm², 6:1 length/width aspect ratio, Nima Technology, Ltd., Coventry, U.K.) at varying temperatures with a compression speed of 5 cm² min^{−1}. Surface pressure measurements were made using a filter paper (Whatman No. 1) Wilhelmy plate. Monolayers of each surfactant were spread from chloroform solutions on the aqueous subphase, and the solvent was allowed to evaporate for approximately 3 min before beginning compression. All isotherms and transfers were carried out under symmetric compression. All subphases were made using ultrapure water (pH ≈ 5.5), and where noted, the subphase pH was adjusted by the addition of sodium hydroxide (ACS reagent, Sigma-Aldrich). Monolayers were transferred at a constant pressure onto clean silicon wafers and mica using the Langmuir–Blodgett (LB) technique with a dipping speed of 2 mm min^{−1}.

Brewster angle microscopy (BAM) and ellipsometry measurements were carried out with an I-Eli2000 imaging ellipsometer (Nanofilm Technologie GmbH, Göttingen, Germany) equipped with a 50 mW Nd:YAG laser ($\lambda = 532$ nm) using a 20 \times magnification with a lateral resolution of 1 μ m. BAM experiments were performed at an incident angle of 53.15° (Brewster angle of water) and a laser output of 50 and 100% (analyzer, compensator, and polarizer were all set to 0). Ellipsometric measurements at the air–water interface were carried out at an incident angle of 50.00° and a laser output of 100%, with the compensator set to 20.00°. The reported thickness is an average of 10 measurements each taken at a different location on the same film and is consistent for multiple samples. The ellipsometric isotherm is reported in terms of $\delta\Delta$, which is independent of the optical model. $\delta\Delta$ is defined as the difference between the ellipsometric angle Δ of the film on the subphase and the subphase alone ($\delta\Delta = \Delta_{\text{film}} - \Delta_{\text{subphase}}$). Measurements were also carried out on LB films deposited onto silicon substrates using an incident angle of 65.00° and a laser output of 1% with the compensator set to 45.00°. To determine the optical thickness of the monolayers at the air–solid interface, the silicon dioxide layer thickness was determined on clean substrates with the following two-box optical model: silicon as the substrate ($n = 4.15$; $\kappa = 0.04$) and silicon dioxide as the layer ($n = 1.46$; $\kappa = 0$), assuming an isotropic film. The same box model was used to determine the

combined thickness of the LB film and silicon dioxide after LB film deposition. All values are reported as average film thicknesses.

Atomic force microscopy (AFM) was carried out using a Nanoscope IIIa MultiMode AFM from Veeco (Santa Barbara, CA). All images were obtained using tapping mode, using V-shaped silicon nitride tips with a nominal spring constant of 0.58 N m^{−1}. Images were analyzed using the NanoScope Analysis Version 1.40 software.

RESULTS AND DISCUSSION

Surface pressure–area isotherms of silicone boronic acids with varying chain lengths (SiBA-10, SiBA-16, and SiBA-69; Figure 1) at the air–water interface are shown in Figure 2, along with

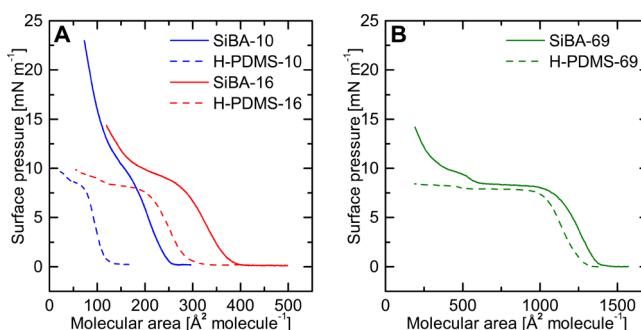


Figure 2. Isotherms for silicone boronic acids and hydride-terminated silicones on ultrapure water at 23 °C: (A) SiBA-10 (solid blue), SiBA-16 (solid red), H-PDMS-10 (dashed blue), and H-PDMS-16 (dashed red) and (B) SiBA-69 (solid green) and H-PDMS-69 (dashed green). Isotherms for the high molecular weight polymer films are displayed separately for clarity given the large difference in molecular area.

isotherms for the corresponding hydride-terminated poly(dimethylsiloxane) precursors (H-PDMS-10, H-PDMS-16, and H-PDMS-69) for comparison. The isotherms for the hydride-terminated PDMS are very similar to those reported for methyl-terminated PDMS,^{2,6,7,9} while those for the silicone boronic acids show similar transitions to other α,ω -difunctionalized PDMS.⁹

In all isotherms, irrespective of the end group (H versus boronic acid), there is a plateau corresponding to a first-order phase transition starting at pressures between 8 and 10 mN m^{−1}, with a slight increase for the low-molecular-weight compounds as previously observed.⁹ Only the molecular areas for transitions and the length of the plateaus vary with chain length. The isotherms for larger molecules have a longer, flatter phase transition plateau, as a result of greater conformational freedom of the chain (i.e., more isoenergetic conformations).

There is the appearance of an additional transition (smaller plateau starting around 550 Å² molecule^{−1}) for the higher molecular weight SiBA-69. Such transitions are commonly observed when the PDMS chain is sufficiently long, in both the presence and absence of end functional groups.⁹ This secondary transition is not limited to silicones and has also been observed in the isotherms of high-molecular-weight, end-functionalized polyisobutylenes.¹² The second transition may also be occurring for the oligomers SiBA-10 and SiBA-16 but may be obscured because the entire isotherm occurs over a much smaller range of molecular areas.

Finally, there is a sharp increase in the surface pressure at low molecular areas for the SiBAs that is not observed for the H-terminal silicones but which is observed for aminopropyl- and other end-functionalized silicones.⁹ This transition must correspond to an additional conformational change for

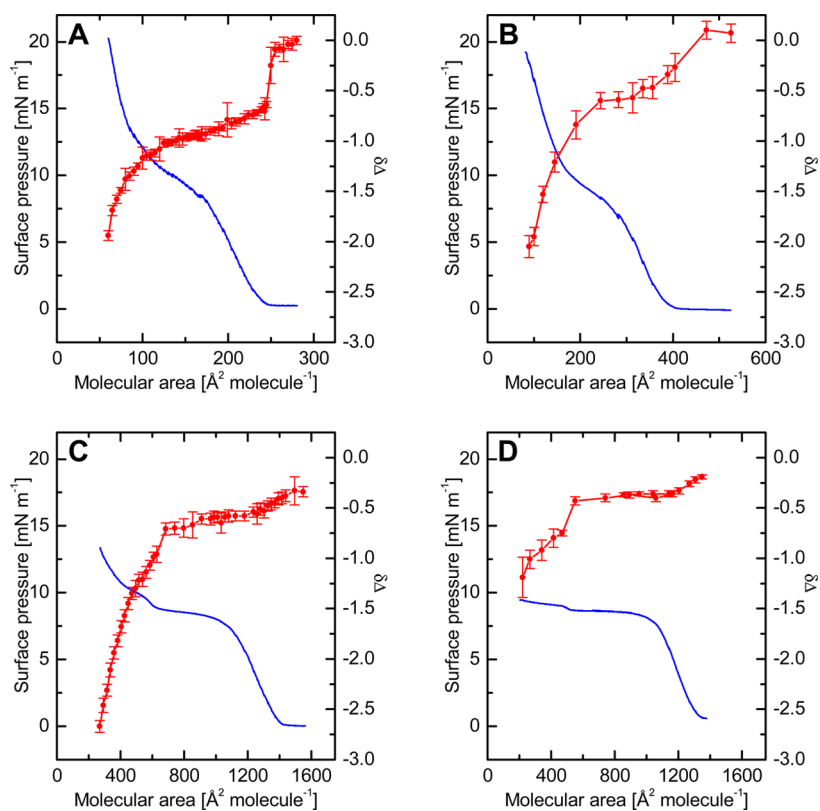


Figure 3. Ellipsometric isotherms at the air–water interface [surface pressure, blue; ellipsometric measurement ($\delta\Delta$), red]: (A) SiBA-10, (B) SiBA-16, (C) SiBA-69, and (D) H-PDMS-69.

molecules that are terminated with polar tethering groups. Without polar end functionalization, the molecules are free to slide over one another as thicker (non-monolayer) organic films are formed, while the surface pressure remains constant. With the polar end functionalization, this migratory layering process is hindered as the molecule is tethered to the subphase. Longer chains may still provide enough flexibility for some layering,^{7,11} but at some point, the tethering limits this process and an alternative conformation is adopted, which leads to a pressure increase at smaller molecular areas (see below). The pressure continues to increase as the film is compressed until a collapsed state is reached at approximately 38–40 mN m^{-1} . The high collapse pressure observed for SiBAs is consistent with strong tethering of the terminal group to the subphase^{9,12} and is comparable to values obtained for amine- and carboxylic acid-terminated PDMS.⁹

BAM images were used to follow film morphology changes throughout the compression isotherms. The formation of very bright domains toward the end of the plateau is attributed to the autophobic dewetting and/or localized collapse of the film (Supporting Information). Autophobic dewetting arises when a fluid cannot spread or wet a thin film comprising the same material;²³ such dewetting processes have been reported for polymer films, such as PDMS, and result in the coexistence of regions of different thicknesses.^{24,25} Schull et al. reported polymer dewetting from a surface-adsorbed (end-tethered) polymer film and noted that this process occurs more readily when the film is tethered at both ends (loops) rather than one end (tails).²³ Dewetting of droplets from a thin film of the same material has been observed for films where the first layer is more ordered than the bulk.²⁵ Given that domains were observed for both the end-functionalized and non-end-

functionalized materials, this must be a property inherent to the silicone backbone that is not impacted by tethering and is attributed to the underlying monolayer being more ordered (zigzag conformation)²⁴ than the overlying layers, which then spontaneously dewet to a lens of disordered material. The dewetting process only occurs after a critical film thickness is achieved, i.e., upon high compression.

Ellipsometric measurements at the air–water interface provide the means to monitor film thickness changes during compression. The ellipsometric isotherms for all three SiBAs are shown in Figure 3, where $\delta\Delta$ is the change in ellipsometric angle Δ and correlates to a change in optical thickness. In all cases, the films show a $\delta\Delta$ of -0.5 just before the critical area for the onset of pressure. This step change in $\delta\Delta$ corresponds to the transition from a backbone caterpillar (Si–O submerged in the subphase) to a zigzag conformation, where the Si–O backbone partially desolvates and forms a thicker film on the surface.⁷ The films then exhibit a slow, progressive increase in thickness (more negative $\delta\Delta$ values) until the end of the plateau, where $\delta\Delta$ reaches approximately -1.0 . For all three SiBA molecules, there is a sharp increase in the average thickness of the film after the plateau (Figure 3D). A much smaller, less drastic increase is observed for H-PDMS-69. The differences between SiBAs and H-PDMSs observed by ellipsometry at these low molecular areas must therefore be attributed to thickness increases as a result of conformational restriction in the underlying SiBA film induced by the boronic acid interaction with the subphase.

The absolute thicknesses of the film below the transition pressure, where the film is homogeneous by BAM, were established by depositing LB films onto silicon wafers. The thicknesses of the deposited films were determined by fitting

ellipsometric angle changes to a two-box model and are shown in Table 2. All three SiBA films have approximately the same

Table 2. Film Thickness of LB-Deposited Monolayers on Silicon Wafers at 5 mN m^{-1} Measured by Ellipsometry at the Air–Solid Interface

surfactant	average film thickness (nm)
SiBA-10	0.5 ± 0.1
SiBA-16	0.6 ± 0.1
SiBA-69	0.6 ± 0.1

thickness, 0.5–0.6 nm; i.e., the thickness is independent of the chain length and correlates well with the thickness determined by Mann and Langevin²⁶ for a PDMS monolayer. This thickness is comparable to the silicone chain dimensions and confirms that the SiBA chains are lying flat at the air–water interface and gradually rise above the surface as the area is compressed, as might be expected for a polymer with a flexible backbone. These observations are quite different from end-functionalized polymers with a less flexible carbon backbone, which were reported to be standing at an angle to the surface and show a defined chain-length dependence.¹²

Ellipsometric measurements on PDMS films by Mann and Langevin revealed an average thickness of 1.4 nm over the phase transition plateau,²⁶ which correlates well with the ellipsometric isotherms (Figure 3) at the air–water interface, showing a significant change in $\delta\Delta$. Ellipsometry measurements on the solid substrate are not reported here for higher pressures given the inhomogeneity of the film. For these systems, AFM

was used to more accurately determine the height differences between the domains and the surrounding film (Figure 4). Films of SiBA-10 were deposited onto silicon and mica from the air–water interface using LB. The films were deposited at surface pressures above the transition plateau (25 mN m^{-1}), where the onset of domain formation (BAM) was observed. The films exhibit the formation of domains of varying lateral and vertical dimensions. Small sub-200 nm domains are distributed throughout the background matrix (note that these domains would not be observed by BAM, which has a limit of resolution of $1\text{--}2 \mu\text{m}$). The majority of these domains vary between 1 and 3 nm above the background film, although a second population of domains with heights from 7 to 11 nm was also observed. Additionally, larger domains of the order of $2\text{--}3 \mu\text{m}$ in diameter were observed; these are likely the domains that are observed by BAM. Upon closer examination, it can be seen that these domains comprise clusters of domains (ranging from 15 to 30 nm above the background film) often surrounded by a thick corona ($2\text{--}7 \text{ nm}$ above the background film). These extremely high domains are likely due to the autophobic dewetting mentioned earlier.

Figure 5 shows isotherms obtained from repeated compression–expansion cycles for SiBA-10 (similar results were also obtained for SiBA-16; Supporting Information) and SiBA-69. Recompression yielded the same isotherm but shifted to smaller molecular areas. This shift was greater when the film was compressed to pressures above the plateau. The isotherms for other bis-end-functionalized silicones have been reported to display little or no hysteresis for molecular weights above 1200

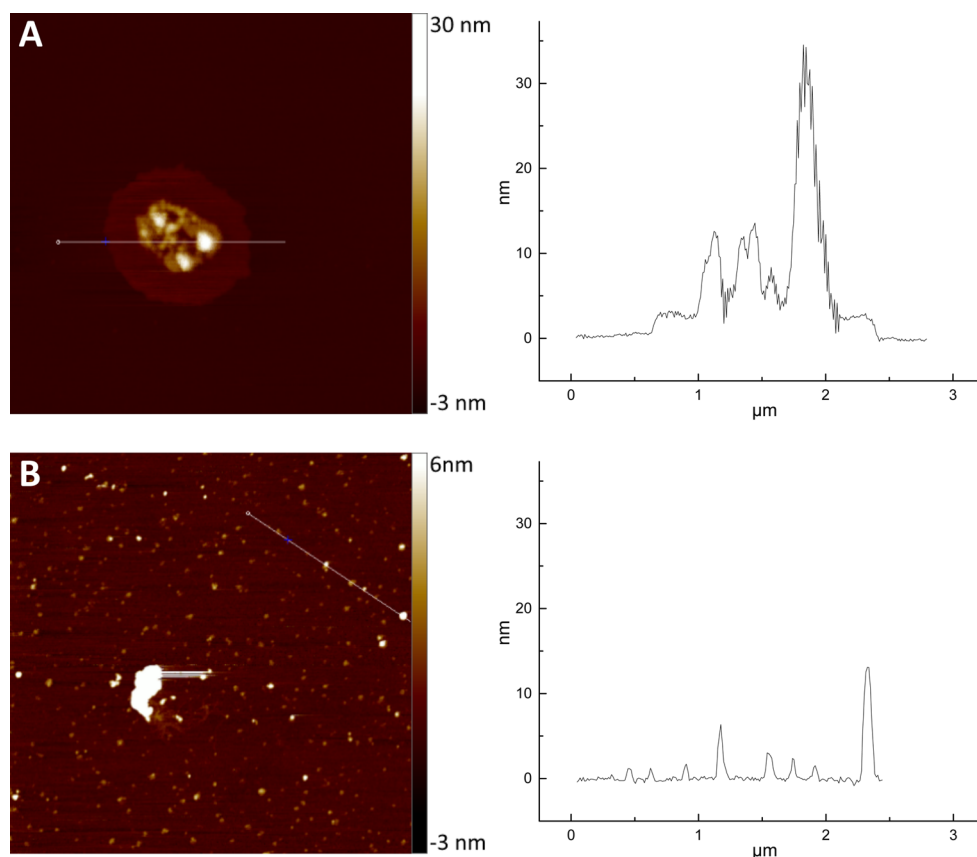


Figure 4. AFM images and corresponding height profiles of SiBA-10 transferred onto a solid substrate at 25 mN m^{-1} : (A) film transferred on mica and (B) film transferred on a silicon wafer. The width of both images is $5 \mu\text{m}$.

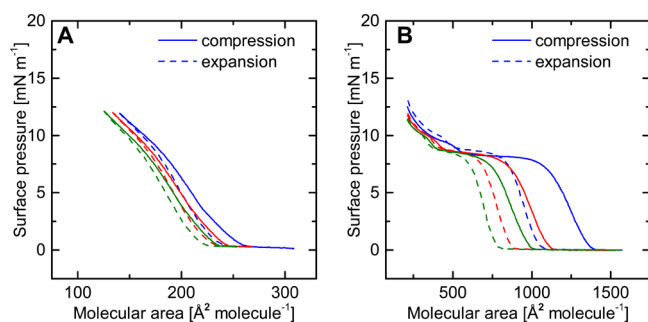


Figure 5. Isotherms for repeated compression–expansion cycles for SiBA films: (A) SiBA-10 and (B) SiBA-69 on water at 23 °C, where solid lines represent film compressions and dashed lines of the same color represent the corresponding film expansion. Recompression starts immediately after expansion without any equilibration time.

g mol^{-1} films,⁹ suggesting that multilayer formation is highly reversible. Additionally, BAM measurements carried out during the repeated compression–expansion cycles showed that the domains, which only become visible at the end of the plateau during the first compression, can still be seen when the film is expanded. During this expansion, the domains lose brightness abruptly; however, they can still be seen below the main phase transition pressure. Upon further expansion into the gaseous phase, the domains are no longer visible because either the multilayer domains have all relaxed or the surface density and/or size of remaining domains is sufficiently low to limit their resolution in the field of view. Upon recompression, the reappearance of these domains occurs even before the phase transition (unlike the first film compression). The greater shifts in the isotherm after multilayer formation for all chain lengths and the BAM measurements suggest that the boronic acid end groups may not be able to readily diffuse away from one another, once in contact, as will be discussed in more detail below.

To further probe the nature of the boronic acid headgroup with the subphase, the pH was varied (Figure 6). The nominal

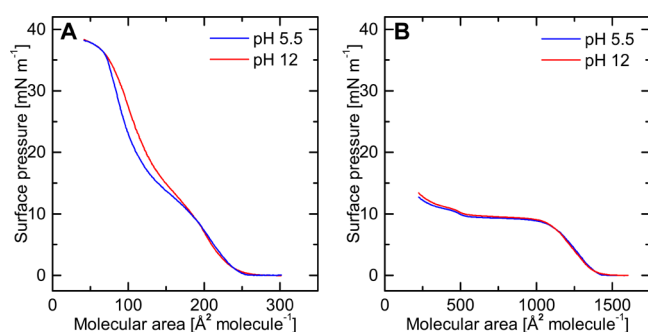


Figure 6. SiBA isotherms on subphases with varying pH: (blue) pH 5.5 subphase and (red) pH 12 subphase. The absolute shift (in $\text{\AA}^2 \cdot \text{molecule}^{-1}$) to higher molecular areas (above the phase transition) with increased pH is similar for both chain lengths but is more prominent in the isotherms for SiBA-10 due to the scale

(solution) $\text{p}K_a$ of boronic acids is ~ 8.9 ,²⁷ the surface $\text{p}K_a$ may be shifted to higher $\text{p}K_a$.²⁸ Furthermore, as a result of the multiple equilibria that exist between the trigonal and tetrahedral (charged) forms of boronic acid and their self-complexed forms, the system may not exhibit a single sharp $\text{p}K_a$ but the charged state may vary over a very broad range of pH values.²⁹ Subphase pH 12 was selected because it is sufficiently

high that the boronic acid headgroups should be predominantly negatively charged, which, in principle, could lead to charge repulsion between the co-localized headgroups and/or disruption of any potential network or dimerization occurring between adjacent boronic acids at the air–water interface, causing an increase in molecular area as was reported for polymerizable surfactants with a boronic acid headgroup (these experiments were undertaken over short reaction times, where essentially no silicone depolymerization is anticipated).²¹ However, for both SiBA-10 and SiBA-69, there was no difference in the isotherm at high molecular areas and low pressures and the shift in the isotherm only becomes apparent at the phase transition.

The observations described above suggest that silicone boronic acids are rather different in their behavior at air–water interfaces from either simple silicones or those bearing hydrophilic functional groups at their termini. When the isotherms for SiBA and H-PDMS are normalized for chain length, as shown in Figure 7, the impact of the boronic acid headgroup becomes much more apparent. It should be noted that the specific area of the functional end group has not been estimated or removed prior to normalization; therefore, the areas per Si–O monomer include an additional area for these headgroups. The isotherms and values for A_0 (the critical area defined by extrapolation of the straight line region of the initial pressure increase to 0 mN m^{-1}) of the polymeric forms and the longest of the oligomers, H-PDMS-16, are comparable to the A_0 of $18.8 \text{ \AA}^2 \text{ molecule}^{-1}$ for methyl-terminated PDMS reported by Kessel et al.,³⁰ including the slight deviation and broadening of the isotherm at low pressure for H-PDMS-16 that was also observed for PDMS with an average chain length of 23 silicon atoms. The normalized isotherm of the shortest oligomer, H-PDMS-10, shifts to significantly smaller areas per molecule. The impact of the smaller terminal group (H versus CH_3) is much greater for a short chain, where the size differences are amortized over a smaller number of repeat units (monomers).

To examine the relative contributions to the molecular area by different headgroups, the normalized isotherms for short-chain oligomers of nine siloxane units with three different terminal functionalities were directly compared. The relative areas occupied by the molecules follow the order: terminal hydride < aminopropyl < phenylboronic acid (Figure 7C). The behavior of aminopropyl-terminated silicone $\text{H}_2\text{N-PDMS-10}$ with its pronounced phase transition corresponds very well to the literature.⁹ The normalized isotherm yields an A_0 value of $17.5 \text{ \AA}^2 \text{ monomer}^{-1}$, which is just slightly less than that of methyl-terminated PDMS, despite the three carbon linker (rather than a methyl group), suggesting that the headgroup orientation is such that the amine must be fully solvated and extending into the subphase. Other end-functional silicones exhibit similar or smaller areas.⁹

For the boronic acid-terminated silicones, only the largest polymeric compound SiBA-69 converges to a monomer critical area of $19 \text{ \AA}^2 \text{ monomer}^{-1}$. This is, in part, because of the lower density of end-functional groups: the longer the chain, the lower the impact of the terminal tethering groups on the conformational changes of the chain and the smaller the proportional contribution of the boronic acid to the molecular area. For the shorter chain oligomeric surfactants SiBA-10 and SiBA-16, A_0 was found to be 28 and $30 \text{ \AA}^2 \text{ monomer}^{-1}$, respectively. Phenylboronic acids are effectively much larger

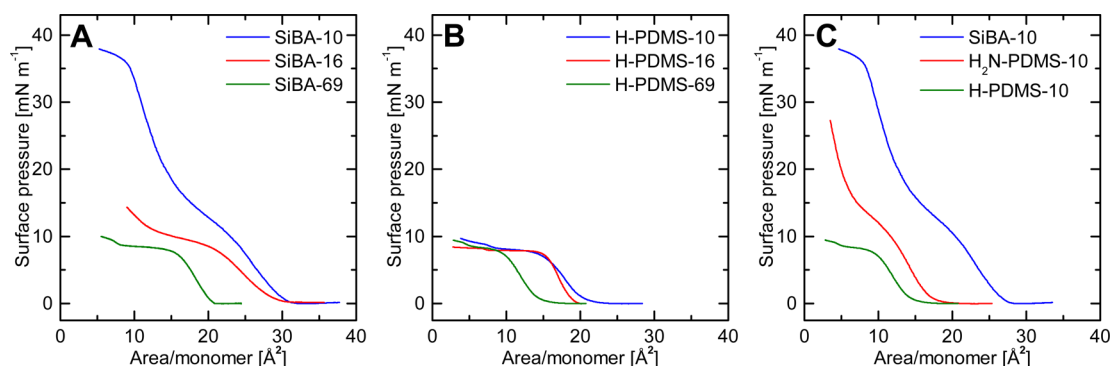


Figure 7. Isotherms normalized for the average chain length and reported as the area per Si–O monomer repeat unit (i.e., $n - 1$): (A) SiBA-10 (blue), SiBA-16 (red), and SiBA-69 (green) and (B) H-PDMS-10 (blue), H-PDMS-16 (red), and H-PDMS-69 (green). (C) Isotherms normalized for chain length for silicones with different terminal functionalities: SiBA-10 (blue), H₂N-PDMS-10 (red), and H-PDMS-10 (green). H₂N-PDMS-10 = aminopropyl-terminated PDMS.

anchoring terminal groups than other functionalities, such as aminoalkyl or carboxyl groups.

To account for these differences, it is necessary to investigate the effect of the end groups separately from the behavior of the silicone backbone. The role of the PDMS backbone is best seen with high-molecular-weight compound SiBA-69. It exhibits many of the characteristics of non-functional PDMS (panels A and B of Figure 8), lying flat as a monolayer (0.5–0.6 nm thick)

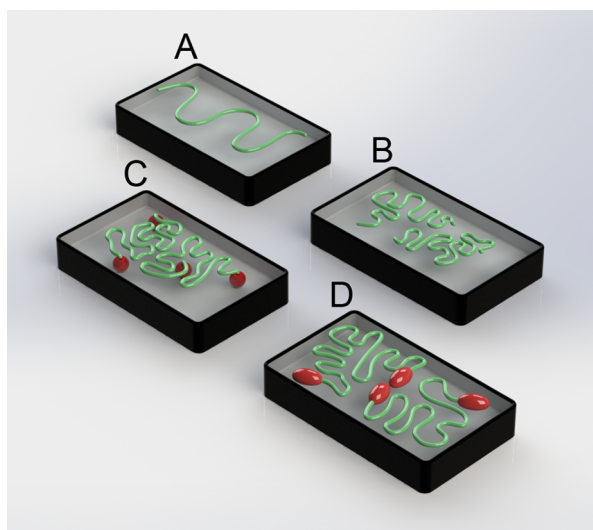


Figure 8. Schematic depictions at the air–water interface of (A) simple silicones at high molecular areas (gas phase), (B) simple silicones upon compression, (C) di-end-functionalized silicones with vertical headgroup orientation observed for most end-functional silicones (e.g., aminopropylsilicones) at all non-zero pressures and for SiBAs at high pressures, and (D) boronic acid-functionalized silicones with horizontal headgroup orientation at low to moderate pressures.

when uncompressed and then increasing in thickness with compression, forming di- to trilayers (1.1–1.4 nm thick). The key distinguishing feature is the larger area that SiBAs exhibit under compression (Figure 8D) when compared to non-functional PDMS, including H-PDMS or end-functional polymers, such as aminopropylsilicones (Figure 8C), which actually take up smaller areas.

Lenk et al. proposed that end-functional silicones, such as aminopropyl or carboxyalkyl compounds are pinned to the

water interface.⁹ The smaller areas occupied by these compounds arise because the polar groups penetrate into the water, which allows for the silicone chains to come into closer proximity (Figure 8C). These differences are magnified with shorter silicones, for which the end groups represent a larger fraction of the molecule. On the other hand, the boronic acid-terminated silicones exhibit significant shifts to higher molecular areas. This can only be accounted for by assuming that the boronic acids do not extend into the subphase. Rather, we propose that they form dimeric structures that lie on the water surface (Figure 8D), a proposal supported by the actual area taken up with boronic acids, which is in the same order of magnitude and range as the estimated area from the molecular dimensions for two phenylboronic acid end groups.

To test this hypothesis, a monofunctional silicone boronate SiBAM was prepared. The isotherms for SiBAM and its mixtures with SiBA-10 are shown in Figure 9. The isotherm of SiBAM displays the same shape as the other SiBAs, with a transition starting at approximately 10 mN m⁻¹, despite the

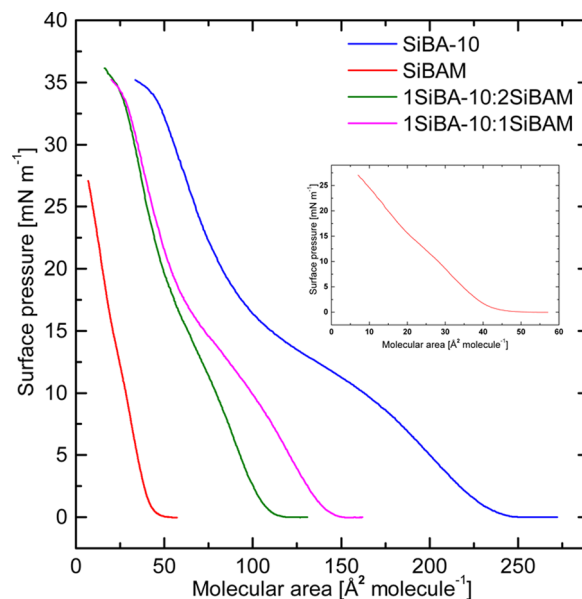


Figure 9. Isotherms of SiBA-10, SiBAM and mixtures of SiBA-10 and SiBAM (1:1 and 1:2 molar ratios, as indicated in the legend). The inset shows an expanded view of the SiBAM isotherm to better see the phase transition.

short chain. The critical area is $43 \text{ \AA}^2 \text{ molecule}^{-1}$, which matches well the cross-sectional area of ethylphenylboronic acid if it were lying flat at the interface (approximately $40 \text{ \AA}^2 \text{ molecule}^{-1}$). A submerged headgroup would be expected to generate a much smaller areal footprint (approximately $16 \text{ \AA}^2 \text{ molecule}^{-1}$). Mixtures of SiBAM with SiBA-10 were prepared in both 1:1 mole and headgroup ratios (the latter being 2 SiBAM molecules/1 SiBA-10 molecule). Both generated isotherms displaying close to ideal mixing behavior ($A_{\text{mix}} = x_{\text{SiBA-10}}A_{\text{SiBAM}} + x_{\text{SiBA-10}}A_{\text{SiBA-10}}$, where x is the mole fraction and A is the area in the single-component isotherm) below the phase transition with a slight positive deviation (indicating repulsive interactions), which increases with increasing amounts of SiBAM.

This orientation may be driven by headgroup complexation: the ability of boronic acids to form dimeric and higher order complexes is well-known and has been exploited as a tool for organization of self-assembled materials.³¹ At the air–water interface, the presence of the Lewis base water can enable this flat dimeric structure, by forming tetracoordinate boron, which is facilitated by relief of angle strain³ and which stabilizes it from substitution compared to the tricoordinate analogue. This configuration (Figure 10) could explain the lack of response to

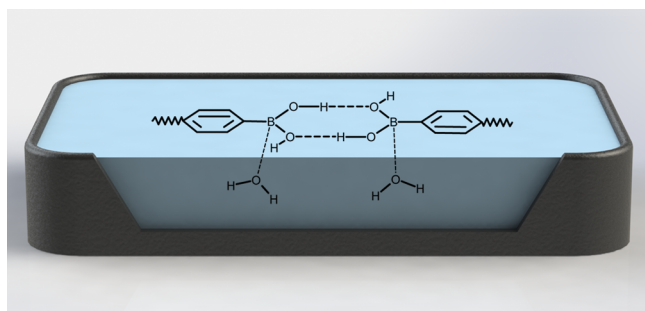


Figure 10. Schematic representation of proposed boronic acid–boronic acid complexation leading to a planar headgroup orientation at the air–water interface.

pH changes in the subphase. Increased basicity would simply pin boron to the water interface more efficiently (Figure 8B). Only at very high pressures can the boron dimer be coerced into extending into the subphase with increased solvation. Such complexation would also explain the hysteresis exhibited by all three SiBAs (not observed for other highly polar end functionalizations): sufficiently strong headgroup interactions could inhibit the complete respreading, an effect that is compounded with each cycle as more headgroups come into contact.

The phenylboronic acids are used to confer chemical sensing and electrical conductivity to thin film coatings^{20–22,32} and are ideal self-assembly building blocks as a result of their propensity for self-complexation, electron deficiency, and coplanar structure. We have demonstrated that these self-organization properties extend to the air–water interface, where headgroup complexation induces a planar orientation at the interface, permitting them to take up more area than either non- or end-functionalized silicones, which can only be disrupted through reorientation at high surface pressures in the absence of agents that compete for boronic acid. This different behavior when compared to other silicone surfactants, in terms of interactions between both the hydrophiles themselves and hydrophiles with water, provides new opportunities to target specific applications

that involve the formation of robust hydrophobic films at aqueous interfaces, including coating applications. Attempts to exploit this behavior will be the subject of future reports.

CONCLUSION

Boronic acid-terminated silicones show behaviors associated with strong tethering of the end functionalization to the subphase. Despite hindering the layering process, tethering does not affect the PDMS autophobic dewetting. However, unlike most bis-end-functionalized PDMS compounds that take up less surface area than PDMS under compression, the SiBAs occupy more space. This is ascribed to planar orientation, possibly induced by boronic acid–boronic acid complexation at the air–water interface, which can only be overcome at much higher pressures that force boronic acids into water.

ASSOCIATED CONTENT

Supporting Information

The Supporting Information is available free of charge on the ACS Publications website at DOI: 10.1021/acs.langmuir.5b02143.

BAM images of SiBA-10, SiBA-69, and H-PDMS-69 (Figure S1) and isotherms for repeated compression–expansion cycles for SiBA-16 (Figure S2) (PDF)

AUTHOR INFORMATION

Corresponding Authors

*E-mail: mabrook@mcmaster.ca.

*E-mail: christine.dewolf@concordia.ca.

Notes

The authors declare no competing financial interest.

ACKNOWLEDGMENTS

The authors thank the Natural Sciences and Engineering Research Council of Canada (NSERC) and 20/20: NSERC Ophthalmic Materials Network for financial support of this research. The authors also thank Heidi Muchall for the determination of molecular dimensions of phenylboronic acids.

REFERENCES

- Buick, R. D.; Buchan, G. D.; Field, R. J. *Pestic. Sci.* **1993**, *38*, 227–35.
- Mehta, S. C.; Somasundaran, P.; Maldarelli, C.; Kulkarni, R. *Langmuir* **2006**, *22*, 9566–9571.
- O'Lenick, A. J., Jr. Silicone sulfate polymers. U.S. Patent 6,777,521 B1, Aug 17, 2004.
- Provasas, A.; Matison, J. G.; Smart, R. S. C. *Langmuir* **1998**, *14*, 1656–1663.
- LaRonde, F. J.; Brook, M. A.; Hu, G. *Silicon Chem.* **2002**, *1*, 215–222.
- Piwovar, A. M.; Gardella, J. A. *Macromolecules (Washington, DC, U. S.)* **2008**, *41*, 2616–2619.
- Kim, C.; Gurau, M. C.; Cremer, P. S.; Yu, H. *Langmuir* **2008**, *24*, 10155–10160.
- Hahn, T. D.; Hsu, S. L.; Stidham, H. D. *Macromolecules (Washington, DC, U. S.)* **1997**, *30*, 87–92.
- Lenk, T. J.; Lee, D. H. T.; Koberstein, J. T. *Langmuir* **1994**, *10*, 1857–64.
- Fox, H. W.; Taylor, P. W.; Zisman, W. A. *Ind. Eng. Chem.* **1947**, *39*, 1401–9.
- Mann, E. K.; Hénon, S.; Langevin, D.; Meunier, J. J. *Phys. II* **1992**, *2*, 1683–704.
- Cox, A. R.; Vincent, B.; Harley, S.; Taylor, S. E. *Colloids Surf., A* **1999**, *146*, 153–162.

- (13) Lee, J.; Joo, H.; Youm, S. G.; Song, S.-H.; Jung, S.; Sohn, D. *Langmuir* **2003**, *19*, 4652–4657.
- (14) Shiino, D.; Murata, Y.; Kubo, A.; Kim, Y. J.; Kataoka, K.; Koyama, Y.; Kikuchi, A.; Yokoyama, M.; Sakurai, Y.; Okano, T. *J. Controlled Release* **1995**, *37*, 269–76.
- (15) Yang, W.; Gao, S.; Gao, X.; Karnati, V. V. R.; Ni, W.; Wang, B.; Hooks, W. B.; Carson, J.; Weston, B. *Bioorg. Med. Chem. Lett.* **2002**, *12*, 2175–2177.
- (16) Springsteen, G.; Wang, B. *Chem. Commun. (Cambridge, U. K.)* **2001**, 1608–1609.
- (17) Springsteen, G.; Wang, B. *Tetrahedron* **2002**, *58*, 5291–5300.
- (18) Dodge, L.; Chen, Y.; Brook, M. A. *Chem. - Eur. J.* **2014**, *20*, 9349–9356.
- (19) Brook, M. A.; Dodge, L.; Chen, Y.; Gonzaga, F.; Amarne, H. *Chem. Commun. (Cambridge, U. K.)* **2013**, *49*, 1392–1394.
- (20) Niwa, M.; Sawada, T.; Higashi, N. *Langmuir* **1998**, *14*, 3916–3920.
- (21) Niwa, M.; Shibahara, S.; Higashi, N. *J. Mater. Chem.* **2000**, *10*, 2647–2651.
- (22) Miyahara, T.; Kurihara, K. *J. Am. Chem. Soc.* **2004**, *126*, 5684–5685.
- (23) Shull, K. R. *Faraday Discuss.* **1994**, *98*, 203–217.
- (24) Bernardini, C.; Stoyanov, S. D.; Cohen Stuart, M. A.; Arnaudov, L. N.; Leermakers, F. A. M. *Langmuir* **2010**, *26*, 11850–11861.
- (25) Reiter, G.; Sharma, A.; Casoli, A.; David, M.-O.; Khanna, R.; Auroy, P. *Langmuir* **1999**, *15*, 2551–2558.
- (26) Mann, E. K.; Langevin, D. *Langmuir* **1991**, *7*, 1112–7.
- (27) Hall, D. G. Structure, properties, and preparation of boronic acid derivatives. Overview of their reactions and applications. In *Boronic Acids*; Hall, D. G., Ed.; Wiley-VCH Verlag GmbH & Co. KGaA: Weinheim, Germany, 2006; pp 1–99.
- (28) Andersson, M. P.; Olsson, M. H. M.; Stipp, S. L. S. *Langmuir* **2014**, *30*, 6437–6445.
- (29) Yan, J.; Springsteen, G.; Deeter, S.; Wang, B. *Tetrahedron* **2004**, *60*, 11205–11209.
- (30) Kessel, C. R.; Granick, S. *Langmuir* **1991**, *7*, 532–8.
- (31) Nishiyabu, R.; Kubo, Y.; James, T. D.; Fossey, J. S. *Chem. Commun. (Cambridge, U. K.)* **2011**, *47*, 1124–1150.
- (32) Eyyapan, M.; Çapan, R.; Erdoğan, M.; Sarı, H.; Uzunoglu, T.; Namlı, H. *J. Mater. Sci.: Mater. Electron.* **2013**, *24*, 3403–3411.